Published in final edited form as:
Structure. 2011 March 9; 19(3): 313–323. doi:10.1016/j.str.2011.01.010.

Two Structural and Functional Domains of MESD Required for Proper Folding and Trafficking of LRP5/6

Jianglei Chen[1,a], **Chia-Chen Liu**[2,a], **Qianqian Li**[1], **Christian Nowak**[2], **Guojun Bu**[2,$], and **Jianjun Wang**[1,$]

[1] Department of Biochemistry and Molecular Biology, School of Medicine, Wayne State University, Detroit, Michigan 48201, USA

[2] Departments of Pediatrics, and Cell Biology and Physiology, Washington University, School of Medicine, St. Louis, Missouri 63110, USA

SUMMARY

How the ER folding machinery coordinates general and specialized chaperones during protein translation and folding remains an important unanswered question. Here, we show two structural domains in MESD, a specialized chaperone for LRP5/6, carry out dual functions. The chaperone domain forms a complex with the immature receptor, maintaining the β-propeller domain in an interaction competent state for EGF-repeat binding. This promotes proper folding of the BP domain, causing a binding switch from the chaperone domain to the escort domain. The escort complex ensures LRP5/6 safe-trafficking from the ER to the Golgi by preventing premature ligand-binding. Inside the Golgi, the BP domain may contain a histidine switch, regulating MESD dissociation and retrieval. Together, we generate a plausible cell biology picture of the MESD/LRP5/6 pathway, suggesting that it is the specialized chaperones, MESD, that serves as the folding template to drive proper folding and safe trafficking of large multi-domain proteins LRP5/6.

INTRODUCTION

Low-density lipoprotein receptor (LDLR) family members control diverse developmental and physiological pathways, including endocytic cargo functions and signaling capacities (Herz and Bock, 2002; Strickland et al., 2002). In the Wnt/Wingless (Wg) signaling pathway, the mammalian LDLR-related proteins 5 and 6 (LRP5/6) are essential co-receptors for binding to Wnts, controlling many aspects of animal development (Huang and He, 2008). Variant LDLRs or their ligands can contribute to several major human diseases, including hypercholesterolemia, atherosclerosis, bone diseases and developmental and neurodegenerative disorders such as Alzheimer's disease. All members of LDLR family belong to type I transmembrane proteins and contain repeating structural modules. The extracellular side contains cysteine-rich repeats (LDL-A) that makes up the ligand-binding domains, a BP domain formed by six YWTD repeats and an epidermal growth factor (EGF)

[$]Correspondences: Tel.: 313-577-8836; jwang@med.wayne.edu. Tel.: 314-286-2860; Bu@kids.wustl.edu.
[a]These authors contributed equally to this work.

repeat. The number and arrangement of these repeats vary dramatically among family members (May et al., 2005; Strickland et al., 2002).

LDLR family members enter the secretion pathway as they are translated by the ER-associated ribosomes. These proteins fold and mature inside the ER and traffic from the ER through the Golgi apparatus to the cell membrane. Effective quality control systems in mammalian cells ensure that only the properly folded proteins can be exported from the ER and the misfolded proteins will be retained in the ER and removed by the ER-associated degradation (ERAD) (Herz and Marschang, 2003). Numerous chaperones and folding enzymes function in the ER to ensure proper folding and maturation of most proteins (Stevens and Argon, 1999), including BiP/PDI, calnexin/calreticulin, as well as various specialized chaperones and escort proteins (Ellgaard et al., 1999). However, how the ER folding machinery coordinates general and specialized chaperones during protein translation and folding remains an important unanswered question in cell biology.

For the LDLR family, two specialized chaperones have been identified. The receptor-associated protein (RAP) is an ER-resident chaperone that is necessary for efficient folding of the ligand-binding domain of some LDLR family members (Bu, 2001). RAP also escorts the receptor from the ER to the Golgi and prevents premature association of ligands (Herz and Marschang, 2003). The X-ray crystal structure of the third domain of RAP complexed with two-LDL-A repeats of LDLR indicates two interaction sites, one for each LDL-A repeat. Each site contains three conserved acidic residues from one LDL-A repeat encircling a lysine side chain from RAP through electrostatic interactions. This “acidic necklace” may represent a general binding strategy for other basic ligands to LDLR family proteins (Fisher et al., 2006). In addition, a histidine switch in RAP has been suggested to regulate its interaction with LRP in the ER and Golgi (Lee et al., 2006).

Another specialized chaperone, termed *mesoderm development* (MESD) in mouse (Hsieh et al., 2003) and *boca* in fly (Culi and Mann, 2003), is essential for Wg/Wnt signaling. MESD/Boca does not function as a direct component of the Wg/Wnt signaling pathway but as a molecular chaperone inside the ER, specifically for the LDLR family, including LRP5/6 (Hsieh et al., 2003). In the absence of MESD, LRP5/6 fail to reach the cell surface and remain sequestered as insoluble aggregates due to misfolding. Boca is specifically required for maturation of the BP domains. It is further suggested that Boca binds to the β-propeller to maintain it in an interaction competent state for EGF repeat binding. Subsequently, upon EGF-binding, the BP domain is able to achieve a more mature state that excludes the binding of Boca (Culi et al., 2004). We previously showed MESD could bind to mature LRP5/6 at the cell surface, which antagonizes Dkk1 binding (Li et al., 2005). We further demonstrated that the C-terminal region, MESD(150–195) is necessary and sufficient for binding to cell surface located, intact LRP6. Another truncation mutant, MESD(12–155), a vertebrate analogue of Boca, fails to bind to the cell surface located, intact LRP6 (Li et al., 2005). The NMR structure of MESD(60–155) showed a structured core region of a four-stranded anti-parallel β-sheet and three α-helices positioned on one side of the sheet (Kohler et al., 2006). Experimental data confirmed this structural core domain, suggesting both the N- and C-terminal unstructured regions are required to facilitate maturation of LRP6 (Koduri and Blacklow, 2007).

We report here the NMR structure of MESD, indicating two structural domains. Mutagenesis and cell biology/functional data indicate each domain is responsible for an independent and specific biological function. While the central core domain is responsible for the chaperone function, the C-terminal flexible helical domain binds to and escorts mature receptors from the ER to the Golgi. We generated a chaperone complex and an escort complex and derived the possible detailed binding interactions. This binding mode is

distinctly different from that of general chaperones; however, it may represent a general binding mode for all specialized chaperones. We also discussed the possible structural switching mechanisms during MESD's chaperone, escort and retrieval cycle between the ER and Golgi.

RESULTS

NMR Structure of MESD contains two distinct structural domains

Figure 1A depicts 20 best-fit NMR structures and Figure 1B shows a ribbon representation of the average structure of MESD (PDB accession code: 2KGL, see NMR restraints and structural statistics in Table 1; the complete resonance assignments were deposited and validated in BMRB with accession code: 16213). The structure contains a four strand anti-parallel β-sheet, surrounded by several α-helices either located above (5 helices) or below (1 red helix) the sheet. Figure S1 shows a sequence alignment of MESD from four different species and the secondary structural locations of MESD based on NMR structure. Together with three long helices, four β-strands form a well-defined core structure. Three short helices, highlighted in pink and blue, are flanked by long loops (Figure 1B). The loops are relatively defined, especially for those loops that connect strands. The RMSD of backbone heavy atoms of the core structural region is 0.43±0.04 Å, whereas the RMSD for all heavy atoms of the same region is 1.17±0.10 Å, indicating a well-converged core structure. The NMR structures are back-calculated and validated using the Protein Structure Validation Suite (PSVS) through BioMagResDB. A good DP-score of 0.791 for the average NMR structure of MESD is obtained (Table S1), suggesting the reliability of this NMR structure of MESD. The Ramachandran analysis results indicate that in the ordered regions of MESD, 73.9% of residues are located in the most favored regions, 22.8% of residues are in the additional allowed regions and 3.3% of residues are in the generously allowed region of the Ramachandran plot. No residues are observed in the disallowed region (Table 1). If all the flexible loop regions are excluded from Ramachandran analysis, 94.2% of residues are located in the most favored regions and 5.8% in the additionally allowed region. No residues are located in the generally allowed and disallowed region, indicating a high-quality well-defined core structure of MESD (Table 1).

The NMR structure of MESD clearly suggests two distinct structural domains: the central core domain (residues 1–155) and a C-terminal flexible helical domain (residues 156–195). We show the core domain in green and the C-terminal flexible helical domain in yellow with the potential interacting residues highlighted (Figure 1C). In the core domain, W32 and H46 are shown as purple sticks, with an additional five lysines, K14, K15, K68, K71 and K72. These residues spread along the edge of the core domain and are solvent exposed, mostly located in the loops (K14, K15, H46, K71 and K72) and flexible helix 2 (K68), except W32 which is located in helix 1. In the C-terminal flexible helical domain, an array of positively charged residue side chains are shown as brown sticks, including K160, K162, K164, K166, K169, K173, K183 and R187. These residues are conserved and fully solvent exposed. They are also located on the same edge and close to those positively charged lysines in the core domain. The electrostatic surface of MESD (Figure 1D) confirms even though these positively charged residues are in different domains, they seem to localize in close proximity, forming a positive surface on one side of MESD (Blue surface).

The secondary and tertiary structures of MESD and its Drosophila orthologs are also compared (see Figures S1 and S2 available online). In figure S1, we compared the secondary structural locations of MESD with the NMR structure of a truncated mutant, MESD(60–155) (Kohler et al., 2006). Generally, secondary structural locations agree well between the two NMR structures with minor variations. In MESD, residues 22–37 form a long helix 1, which has extensive interactions with helix 2 and the C-terminal domain

containing residues 156–195. The C-terminal domain of MESD forms two flexible helices, helices 5 and 6, interacting with helices 1 and 2 in the N-terminal part of MESD. We recently also determined the NMR structure of MESD(12–155), which is the most conserved domain of MESD across different species (Figure S2) (Chen et al., 2010). While MESD(12–155) and MESD adopt a similar tertiary structure, MESD(60–155) displays a major tertiary structural difference (Figure S2). In MESD(60–155), three helices, colored in purple, red and pink, are on the top of the β-sheet (Figure S2A). In contrast, only two helices (purple and pink) on the top, whereas the red helix is under the sheet in both MESD(12–155) and MESD (Figure S2B and S2C). Instead, an N-terminal helix between residues 22–37 (brown) is located on the top of the sheet in MESD and MESD(12–155). This helix is missing in MESD(60–155), however, it is functionally important since it contains the critical residue, W32 (Culi and Mann, 2003). The absence of this crucial helix in MESD(60–155) may be the reason for the tertiary structural difference between MESD and this mutant. The structure of MESD(12–155) is conserved in MESD with noticeable structural difference of helix 2 (residues 64–69) due to the domain-domain interactions, as evidenced by many inter-domain NOEs observed between helix 2 and the C-terminal flexible domain, residues 156–195 (Figure S3 for an example).

MESD's Central Core Domain is the Chaperone Domain

The two-domain structure of MESD raises an important question about the functional relevance of each domain. The structural features of the conserved positively charged residues in domains allow us to speculate the functional importance of these residues. We mutated them to alanines and performed structural and functional characterizations of these mutants. The ^{1}H-^{15}N HSQC spectra of several representative KtoA mutants show no major structural changes. We generated a HA-tagged soluble LRP6 containing all four BP domains (BP1234) (Liu et al., 2009) and performed a secretion assay. As expected, co-expression of wild-type MESD enhanced folding and secretion of BP1234 into the medium (Figure 2A). Significantly, the enhancement of BP1234 secretion was eliminated when co-expressed with MESD_W32R, MESD_W32A, or MESD_H46A, indicating that the chaperone function of these MESD mutants is completely abolished (Figure 2B and 2D). Similarly, the folding and secretion of BP1234 was also partially disrupted when co-expressed with MESD_K68A, K14A/K15A and K71A/K72A mutants (Figure 2D). In contrast, the BP1234 secretion level mediated by MESD_R111A, R118A, or R124A mutants remain the same as that of the wild-type MESD, suggesting these mutations do not disturb the chaperone function (Figure 2C and 2D). These results demonstrate that residues W32, H46, K14, K15, K68, K71 and K72 are crucial for the chaperone function of MESD. Interestingly, these residues are located in the same surface of MESD, whereas R111, R118 and R124 are located on the opposite surface, suggesting that the W32-containing surface is the potential binding surface for the chaperone function (Figure 1D). To investigate whether these residues also play a role in the escort function, we performed a cell surface-binding assay to measure the binding between MESD mutants and cell surface located, mature intact LRP6. Our data indicated that excess unlabeled MESD mutants, exhibiting impaired chaperone function, inhibited ~ 90% of ^{125}I-MESD binding to cell surface LRP6 which is identical to the unlabeled wild-type MESD (Figure 2E). This indicates that none of the residues in the central core domain are important for binding to mature, cell surface located, intact LRP6. Thus, our results suggest that the central core domain is a specialized chaperone domain of MESD.

Since the X-ray crystal structure of the BP domain of LDLR has been solved (Jeon et al., 2001), we aligned four different BP domains of LRP6 against the BP domain of LDLR (Figure S4, upper panel), indicating conserved YWTD motifs. We built a model structure of the first BP domain of LRP6 and carried out docking experiments using the functional data as the restraints, assuming the critical residues for the MESD's chaperone function are

directly involved in binding. Two different views of the chaperone complex are shown (Figure S4, Low Panel). On the left, MESD is shown in surface representation, whereas the BP domain is shown in yellow ribbon with the YWTD motif highlighted in green, indicating the YWTD motifs are involved in the protein-protein interfaces. On the right, MESD is shown in the same surface representation, whereas only the possible interacting residue side chains of the BP domain are shown as yellow sticks and labeled in cyan. The critical residues in MESD are shown as blue sticks and labeled in red. The positively charged lysines in MESD chaperone domain are surrounded by an array of negatively charged residues (Glu and Asp) or polar residues (Asn and Gln) in the BP domain. Interestingly, residue W32 flanked by conserved Q31 and D35 in MESD is close to conserved R9 and R13 (blue sticks) in the BP domain.

Possible Interacting Modes of the Chaperone Complex

Using the critical functional residues in the chaperone domain as restraints, we generated a complex of MESD chaperone domain and the BP domain using molecular docking technique. This complex serves as interacting model of MESD chaperone function (Figure 3A), in which the chaperone domain of MESD adopts a rigid structure that interacts with BP domains through multiple electrostatic binding sites, possibly serving as the potential folding template to ensure BP domain properly folding. Interactions around W32 are centered at R9 of the BP domain (Figure 3B), forming a reverse “acidic necklace” (Fisher et al., 2006; Sivashanmugam and Wang, 2009) with Q31, W32 and E35. The positively charged side chain of R9 forms a salt bridge with D35 and two H-bonds with the side chain carboxylate oxygen of Q31 and the backbone carbonyl oxygen of W32. The aromatic ring of W32 packs against the aliphatic portion of the R9 side chain. Another conserved arginine, R13, also forms a salt bridge with D35 and an H-bond with Q31. Mutations of W32 may destroy this binding pocket, abolishing the chaperone function (Culi and Mann, 2003). For residue H46, we notice that it is in close proximity to the conserved H207 of the BP domain (Figure 3C). The planar aromatic side chains of these two histidine residues stack closely against each other, forming a potential aromatic bridge or πelectron stacking (Noll et al., 2007). K183 of the BP domain may also play a role to stabilize this interaction. Mutation of H46 to Ala destroys this aromatic bridge, causing MESD to lose its chaperone function. Figure 3D shows a zoomed-in view of the interactions between K13 and K15 of MESD and E32/D33/D50/E53 of the BP domain. D50 is in the second YWTD motif. This acidic necklace is centered at K15, with K13 pointing to the same direction as K15, whereas K14 points to the opposite direction. The negatively charged residues in the BP domain form an extensive salt bridge network with K13/K15. However, this binding pocket lacks a Trp/Phe residue, making it an imperfect necklace. Figure 3E shows a zoomed-in view of the binding between K68 of MESD and D94/E96/N98/W115/E117 of the BP domain, as well as the binding between K71/K72 of MESD and Q120/D137/W138/G139/E140 of the BP domain. D94 and D137 belong to the third and fourth YWTD motifs, respectively. For K68, residues D94/E96/N98/W115/E117 of the BP domain form a binding pocket, with three salt bridges and one H-bond. Together with W115, they form a necklace conformation. For K71/K72, centered at K72, residues Q120/D137/W138/G139/E140 of the BP domain form another binding pocket of two salt bridges, two H-bonds and a hydrophobic interaction with W138. K71 forms a salt bridge with E140 and two H-bonds with Q120 and G139. These interactions allow MESD to serve as a chaperone template for the proper folding of the BP domain.

MESD’s C-terminal Flexible Helical Domain is the Escort Domain

To dissect the function of MESD’s C-terminal domain, we mutated the conserved lysine and arginine residues to alanines in the C-terminal flexible helical domain (Figure 4A). The same secretion assay and cell surface binding assay were carried out. Initial results of the

single KtoA mutants showed no difference between the mutants and wild-type MESD in both assays (data not shown). We then prepared an array of multiple KtoA mutants, including double, triple and various other multiple mutants. In particular, we prepared a mutant that replaced all the Lys/Arg residues in this domain with alanines (noK MESD mutant). The results from cell surface binding assays indicate MESD gradually loses its binding capability to mature, cell surface located, intact LRP6 when more mutations are introduced and the noK MESD mutant completely abolished the binding (Figure 4B). A surface binding assay has also been carried out using two different concentrations of the noK MESD mutant and confirmed the same result (Figure 4C). Since the cell surface located intact LRP6 represents the mature and properly folded LRP6, this binding assay recapitulates the escort capability of MESD. To test if these Lys/Arg residues are also involved in the chaperone function, we performed a secretion assay. Our results indicate they play no role in the chaperone function. For example, no difference is observed when the secretion assay results of wild-type and the noK MESD mutant are compared (Figure 4D and 4E). This allows us to suggest that the C-terminal flexible helical domain is a specialized escort domain. Our results also demonstrate the two structural domains of MESD perform independent chaperone and escort functions.

Possible Interacting Modes of the Escort Complex

Using the critical Lys and Arg residues in the escort domain as the restraints, we carried out docking experiments to build an escort complex (Figure 5A). Unlike the chaperone complex, MESD interacts with BP domains in the escort complex through a cluster of positively charged residues on its flexible C-terminal tail. For the K162/K164 pair, the acidic necklace is formed by E117/D119/Q120/D137/W138/G139/E140 of the BP domain, which is centered at K164, forming three salt bridges with E117, D119 and D137 (Figure 5B). Two H-bonds are also possibly formed between K164 of MESD and Q120 and N98 of the BP domain. The side chain of W138 is tightly packed against the aliphatic side chain of K164. K162 forms a salt bridge with E140 and an H-bond with the backbone carboxylate oxygen atom of G139. For the K166/K169 pair, the binding seems to be centered at K166, which forms three salt bridges with D79, E96 and E117 (Figure 5B). An additional H-bond is possibly formed between K166 and N98. For K169, three salt bridges are formed with D79, D94 and E96. No Trp residues can be found in proximity of K166/K169. Among all the binding residues in the BP domain, D94/D137 are part of YWTD motifs and D79, N98, E117, D119, W138, G139 and E140 are conserved residues (Figure S4). The acidic necklaces for K173, K183 and R187 in MESD are formed by E32/D33/D50/E53/E54 of the BP domain (Figure 5C). These negatively charged residues form an extensive salt bridge network with K173, K183 and R187, enhancing the binding between the escort domain and the BP domain. D50 is a residue of the second YWTD motif and D33/E53 are conserved residues. Their interactions with the lysine residues are likely essential for this binding pocket.

DISCUSSION

Our data clearly indicates that MESD contains two structural/functional domains: a chaperone domain and an escort domain. Mutations in one domain only impair the function of this domain without affecting the function of the other domain. These results explain the fact that MESD(150–195), which is the escort domain, is able to bind to the mature, intact LRP6 on the cell surface with a similar binding affinity of full-length MESD (Li et al., 2005). The NMR structure of an inactive truncation mutant, MESD(60–155), showed a significant different tertiary structure from the NMR structures of both active MESD(12–155) and MESD (Figure S2), since 1/3 of the chaperone domain was truncated in MESD(60–155) (Kohler et al., 2006). It is well-established that different truncation mutants

of the same protein may display different tertiary structure. However, the proper truncation mutant, MESD(12–155), maintains the entire chaperone domain, thus displaying a similar tertiary structure and maintaining the chaperone function of MESD. The structural similarity between MESD(12–155) and MESD confirms the two domain structure of MESD that is essential for the dual functions of this protein. Furthermore, we successfully design and identify functionally-important mutations in both domains that are critical to MESD's chaperone and escort functions, based on this NMR structure. As a result, our functional results of these rationally designed MESD mutants confirmed the structural insights revealed by the NMR structure, provide the additional approaches to validate the NMR structure of MESD.

The interactions in both chaperone and escort complexes belong to typical acidic necklaces (Fisher et al., 2006). However, exceptions do exist. For example, conserved R9 and R13 of the BP domain provide positively charged residues, whereas Q31, W32 and D35 on helix 1 of MESD form a reverse acidic necklace. The W32R mutation of *boca* is the *boca*^{1} allele, which is a loss-of-function mutation (Culi and Mann, 2003). Mutations of W32 destroy the reverse acidic necklace, causing loss of chaperone function (Figure 3B). The second example is H46, which forms an aromatic bridge with conserved H207 of the BP domain. A mutation with an alanine removes this aromatic bridge, causing loss of chaperone function (Figure 3C).

An LRP5 high-bone-mass G171V mutation disrupts LRP5 interaction with MESD (Zhang et al., 2004). Upon removing the signal peptide, G171 is equivalent to G139 of LRP6. Careful examination of both chaperone and escort complexes indicates G139 is part of the acidic necklaces and its backbone carbonyl oxygen forms an H-bond with a lysine residue in MESD in both complexes. The limited space of the acidic necklaces for K71/K72 in the chaperone complex (Figure 3E) and for K162/K164 in the escort complex (Figure 5B) only allows a glycine to fit well into this necklace. A G139V mutation may impose a large stereo hindrance that destroys these acidic necklaces, disrupting the MESD binding in both complexes. Thus, both chaperone and escort complexes provide the structural basis for the malfunction in MESD-binding of this high-bone-mass G171V mutation of LRP5.

Culi and co-workers postulated if a β-propeller requires an EGF repeat to traffic through the secretion pathway, it also requires Boca. Boca maintains the β-propeller domain in an interaction competent state. Subsequently, once the EGF repeat is translated, the β-propeller interacts with the EGF repeat to achieve a more mature state, thereby removing the Boca binding from the BP domain due to a lower affinity (Culi et al., 2004). A major difference between MESD and Boca is that Boca only contains the chaperone domain of MESD and lacks the escort domain. If a BP domain releases Boca after cooperative folding with the EGF repeat, one may argue that this mature BP domain also releases the chaperone domain of MESD under the same situation. The question remains as to how the binding of the chaperone domain of MESD or Boca maintains the β-propeller in an interaction competent state?

Our chaperone complex may provide an answer (Figure 6A). The binding interface of the chaperone complex is at one end of the BP domain that contains the YWTD motifs. Five major binding sites are around the outside edges of the complex to completely cover the YWTD-end, serving as an ideal folding template for the YWTD-end of the BP domain. We suggest that the YWTD-end is likely the end that the BP domain binds to the physiological ligands of LRP5/6, such as Wnt and Dkk1. The binding of the chaperone domain prevents premature binding of these physiological ligands. It also prevents the newly synthesized EGF repeat from binding. Subsequently, the EGF repeat can only bind to the opposite end, which contains a large hydrophobic face (brown), making the β-propeller itself unstable,

likely to interact with another BP domain to form oligomers, or interact with the newly synthesized EGF repeat which also contains a large hydrophobic face (lemon) (Figure 6A). In this sense, the binding of the chaperone domain to the YWTD-end not only provides a folding template, but also maintains the β-propeller in an interaction competent state. The binding of the newly translated EGF repeat to this large hydrophobic face makes the β-propeller stable, promoting the β-propeller domain to cooperatively fold with the EGF repeat. This allows the mature state of the properly folded BP domain to be achieved.

Once the BP domain becomes properly folded, MESD has to switch its binding from the chaperone domain to its escort domain. An important question remains: how does this switch happen inside the ER? Culi et al. suggested in the absence of an EGF repeat, LpR2_β exists in an immature state that binds to Boca. When an EGF repeat is present, as in LpR2_β/E3, the βpropeller reaches a mature state that has a lower affinity for Boca (Culi et al., 2004). Thus, the folding states of the BP domain itself may provide a switch. When unfolded/misfolded, the BP domain requires the chaperone domain of MESD for folding/refolding. After the BP domain is properly folded, this mature BP domain disfavors the binding with either Boca or the chaperone domain of MESD, thus releasing them from the BP domain.

Upon release of the chaperone domain in the ER, MESD binds to the mature BP domain through its escort domain to form the escort complex. The potential escort complex (Figure 6B) shows that the binding of the escort domain only covers half of the YWTD-end, including YWTD2, YWTD3 and YWTD4 (green). Since the escort domain is encircling only half of the YWTD-end and it is much more flexible, this binding mode is a more favorable binding mode for the mature BP domain and introduces less stereo hindrance for the packing of different BP domains. The other half of the YWTD-end, including YWTD1, YWTD5 and YWTD6 (brown), contains three histidine residues H207, H226 and H243 in the binding interface (space-filling model). A fourth histidine, H46 of MESD, is also in this region. These histidine residues are not positively charged at the neutral pH inside the ER.

We suggest that these histidine residues may serve as a histidine switch that regulates the escort complex formation and dissociation in the ER and Golgi. Inside the Golgi, histidine residues become positively charged due to the acidic environment (Demaurex, 2002), repelling the interface-located, positively charged lysine residues of MESD and causing dissociation of the escort complex. This ensures MESD is recycled back to the ER, whereas the mature receptor will be properly post-translationally modified inside the Golgi and further travel to the cell surface. Different from RAP, this histidine switch is provided by the receptor, indicating the BP domain plays a central role in mediating its interaction with MESD between the ER and Golgi. Among the three histidines, only H207 is conserved (Figure S4), suggesting the diversity of the BP domains in LRP5/6. Each BP domain may display different switching mechanisms. Our recent finding of cooperative folding and ligand-binding properties of the BP domains of LRP6 supports the diversity of the BP domain (Liu et al., 2009). A cell biology picture of the MESD/LRP5/6 pathway (Figure 7) suggests that it is the specialized chaperone MESD that determines proper folding of the BP domain of LRP5/6, whereas the BP domain strategically regulates structural switches of the two structural domains of MESD in a unique fashion to ensure both proper folding and safe trafficking of the receptor along the secretory pathway, as well as the ER-retrieval of MESD protein. Our results further suggest that the escort function may be a recent evolutionary acquisition of these chaperones, since Boca, the Drosophila ortholog of MESD, lacks the C-terminal escort domain.

Large proteins, like LRP5/6, composed of multiple domains, often fold inefficiently inside the ER due to the formation of partially folded and misfolded intermediates that tend to

aggregate (Hartl and Hayer-Hartl, 2002). The ER folding machinery utilizes general chaperones to counteract the aggregation during both *de novo* folding and refolding under stress conditions (Hartl and Hayer-Hartl, 2002). The typical target of general chaperones is a short unstructured stretch of hydrophobic amino acids flanked by basic residues and lacking acidic residues (Baneyx and Mujacic, 2004). Binding of general chaperones favors this on-pathway folding by shielding interactive hydrophobic surfaces from each other and from the intracellular environment, preventing aggregation and premature folding as protein chain elongation proceeds. Once the protein domain is translated, the general chaperones release an unfolded protein chain (Hartl and Hayer-Hartl, 2002).

Our results show that the specialized chaperones, such as MESD, act differently. First, the binding mode is different. While general chaperones bind to the substrate through less specific hydrophobic interactions, MESD binds to LRP6 through acidic necklaces and aromatic bridges. These are specific interactions, which require the interacting residues at specific positions in both proteins, driving the BP domain of LRP6 to a specific position of MESD. These specific binding features and the rigidity of the chaperone domain of MESD make it ideal to serve as a folding template for proper folding of the BP domain of LRP6. During LRP6 translation, once the binding residues in the BP domain are synthesized, they will immediately bind to the specific residues of MESD *via* salt bridges and H-bonds. This binding mode prevents both premature binding of the physiological ligand and the binding of the EGF repeat. The binding of the subsequently translated EGF repeat to the large hydrophobic face on the opposite end of the YWTD-end makes the β-propeller stable, causing it to cooperatively fold with the EGF repeat.

The second major difference is the folding states of the substrate. Upon release from a general chaperone (except chaperonin), the substrate protein remains unfolded and it still has to undergo a folding process to achieve a biologically active conformation. However, the chaperone domain of MESD only releases the properly folded substrate. This indicates that it is the specialized chaperone like MESD that serves as the folding template for large multi-domain proteins and guides the different modules to bind to the correct places so that the multiple modules can fold cooperatively. Therefore, the specialized chaperones for a particular protein or protein family serve as the “true chaperones”. In contrast, the main mission of general chaperones in the ER folding machinery seems to allow for nascent chain elongation until sufficient sequence, such as a domain, is available for correct folding to occur. In this sense, the general chaperones are only “transient chaperones”, since they do not directly promote the proper folding of multi-domain proteins or a protein family. Therefore, we further suggest that large multi-domain proteins may be required to have specialized chaperones for their proper folding and functions. In contrast to the general chaperones that are regulated in a complex ATP-dependent manner for their binding and release of substrate proteins, MESD does not require this ATP-dependent regulation. In addition, MESD also serves as an escort protein *via* the formation of an escort complex. Thus, our results provide the structural mechanism for how the ER folding machinery coordinates general chaperones and MESD during LRP5/6 translation, folding and intracellular trafficking.

EXPERIMENTAL PROCEDURES

Materials

The preparation of recombinant MESD protein was described previously (Li et al., 2005). Anti-Flag antibodies (Sigma), and anti-actin antibodies (Sigma) were used according to manufacturers’ instructions.

Cell culture and transfection

LRP6-transduced HT1080 cells have been described before (Li et al., 2004), and were cultured in Dulbecco minimum essential medium (DMEM) containing 10% fetal bovine serum (FBS) and 350 μg/ml G418. BHK570 were cultured in DMEM supplemented with 10% FBS and 1% L-glutamine, and maintained at 37°C in humidified air containing 5% CO_2. For transient transfection, BHK570 cells were transfected with various plasmids at 90% confluence using lipofectamine 2000 according to manufacturers' instructions.

Generation of LRP6 BP1234 construct

Human LRP6 cDNA (kindly provided by Dr. Christof Niehrs, Deutsches Krebsforschungszentrum, Heidelberg, Germany) was used as the template for PCR. HA-tagged LRP6 BP1234 (consisting of the four BP domains) was constructed by subcloning PCR products into the BamH1/XbaI sites of mLRP4T100 backbone whose construction has been described previously (Bu and Rennke, 1996). Construct derived from PCR was confirmed by sequencing.

Western blotting

BHK570 cells were transiently transfected with HA-tagged LRP6 BP1234 with the co-transfection of either pcDNA, or Flag-tagged MESD wild type or mutants. Six hours later, culture media were replaced with DMEM supplemented with 1% FBS and the secretion of BPs proceeded for 48 h. Cells were lysed at 4 °C for 30 min, and culture media were concentrated with Centricon YM-30 (Millipore) at 4 °C. Equal quantities of protein were subjected to SDS-PAGE under reducing conditions. Following transfer to Immobilon-P transfer membrane, successive incubations with indicated primary and horseradish peroxidase-conjugated secondary antibodies (Amersham Life Science) were carried out. The immunoreactive proteins were then detected using the ECL system.

Cell surface binding

LRP6-transduced HT1080 cells were plated in 12-well plates at a density of 2×10^5 cells/well and used after overnight culture. Cells were rinsed twice in ice-cold ligand binding buffer (DMEM containing 6 mg/ml bovine serum albumin), and ^{125}I-MESD was added at 5 nM final concentration in cold ligand binding buffer in the absence or the presence of 50 nM or 100 nM unlabeled wildtype MESD or mutants (0.5 ml/well). The binding of ^{125}I-MESD was carried out at 4°C for 2 h with gentle rocking. Thereafter, unbound ^{125}I-MESD was removed by washing cell monolayers three times with cold PBS. Cells were then lysed in 1N NaOH and radioactivity was counted. The protein concentration of each cell lysate was measured in parallel dishes that did not contain the MESD ligands.

NMR spectroscopy and structure determination

The NMR sample contained 1 mM isotope-labeled MESD protein, 25 mM sodium phosphate at pH 6.8, 0.01 mM NaN_3, 10 mM EDTA, 50 mM d_{10}-DTT, 0.03 mM DSS and 5% D_2O. All spectra were acquired at 30 °C on 600 MHz Varian INOVA spectrometer equipped with a cryogenic probe. 3D-HNCA, HN(CO)CA, HN(CA)CB, HN(COCA)CB spectra were used for backbone atom assignment while HCC-TOCSY-NNH, CCC-TOCSY-NNH, ^{15}N-edited NOESY and 4D-^{13}C^{15}N-edited NOESY were collected for the sidechain atom assignment. The NMR data was processed using nmrPipe (Delaglio et al., 1995), and analyzed on a SGI workstation using nmrview (Johnson, 2004). TALOS program was used to obtain the backbone dihedral angles (φ and Ψ(Cornilescu et al., 1999). NOE distance restraints were generated using 3D/4D Nuclear Overhauser Effect Spectroscopy (NOESY) experiments, including ^{15}N-edited NOESY and 4D-^{13}C^{15}N-edited NOESY. A total of 264 dihedral angle constraints, 1646 distance constraints and 75 constraints for hydrogen bonds,

were used as input for CYANA calculations (Guntert, 2004). Two hundred structures were generated and energy minimized in CYANA, including 10,000 steps of simulated annealing. Final NMR structures were analyzed using InsightII (MSI, San Diego).

Homology Structural Building and Docking

The homology structure of the first BP domain of LRP6 was generated by homology structural modeling using the ESyPred3D (Lambert et al., 2002), based on the structure of the BP domain of the LDLR (Jeon et al., 2001) and sequence alignment between the BP domains of LDLR and LRP6. Insight II (MSI, San Diego) was used for manual docking of MESD and the BP domain using the functional data of the mutants as the restraints during docking. The electrostatic potential was calculated using APBS (Baker et al., 2001) and displayed using Pymol (DeLano Scientific, Palo Alto).

Supplementary Material

Refer to Web version on PubMed Central for supplementary material.

Acknowledgments

This work is supported by NIH RO1 grants (HL 074365 and HL 076620 to JW and AG027924 to GB). The authors also thank Ms Victoria Murray for critical reading of the manuscript.

References

Baker NA, Sept D, Joseph S, Holst MJ, McCammon JA. Electrostatics of nanosystems: application to microtubules and the ribosome. Proc Natl Acad Sci U S A. 2001; 98:10037–10041. [PubMed: 11517324]

Baneyx F, Mujacic M. Recombinant protein folding and misfolding in Escherichia coli. Nat Biotechnol. 2004; 22:1399–1408. [PubMed: 15529165]

Bu G. The roles of receptor-associated protein (RAP) as a molecular chaperone for members of the LDL receptor family. Int Rev Cytol. 2001; 209:79–116. [PubMed: 11580203]

Bu G, Rennke S. Receptor-associated protein is a folding chaperone for low density lipoprotein receptor-related protein. J Biol Chem. 1996; 271:22218–22224. [PubMed: 8703036]

Chen J, Li Q, Liu CC, Zhou B, Bu G, Wang J. NMR structure note: solution structure of the core domain of MESD that is essential for proper folding of LRP5/6. J Biomol NMR. 2010; 47:283–288. [PubMed: 20506034]

Cornilescu G, Delaglio F, Bax A. Protein backbone angle restraints from searching a database for chemical shift and sequence homology. J Biomol NMR. 1999; 13:289–302. [PubMed: 10212987]

Culi J, Mann RS. Boca, an endoplasmic reticulum protein required for wingless signaling and trafficking of LDL receptor family members in Drosophila. Cell. 2003; 112:343–354. [PubMed: 12581524]

Culi J, Springer TA, Mann RS. Boca-dependent maturation of beta-propeller/EGF modules in low-density lipoprotein receptor proteins. Embo J. 2004; 23:1372–1380. [PubMed: 15014448]

Delaglio F, Grzesiek S, Vuister GW, Zhu G, Pfeifer J, Bax A. NMRPipe: a multidimensional spectral processing system based on UNIX pipes. J Biomol NMR. 1995; 6:277–293. [PubMed: 8520220]

Demaurex N. pH Homeostasis of cellular organelles. News Physiol Sci. 2002; 17:1–5. [PubMed: 11821527]

Ellgaard L, Molinari M, Helenius A. Setting the standards: quality control in the secretory pathway. Science. 1999; 286:1882–1888. [PubMed: 10583943]

Fisher C, Beglova N, Blacklow SC. Structure of an LDLR-RAP complex reveals a general mode for ligand recognition by lipoprotein receptors. Mol Cell. 2006; 22:277–283. [PubMed: 16630895]

Guntert P. Automated NMR structure calculation with CYANA. Methods Mol Biol. 2004; 278:353–378. [PubMed: 15318003]

Hartl FU, Hayer-Hartl M. Molecular chaperones in the cytosol: from nascent chain to folded protein. Science. 2002; 295:1852–1858. [PubMed: 11884745]

Herz J, Bock HH. Lipoprotein receptors in the nervous system. Annu Rev Biochem. 2002; 71:405–434. [PubMed: 12045102]

Herz J, Marschang P. Coaxing the LDL receptor family into the fold. Cell. 2003; 112:289–292. [PubMed: 12581519]

Hsieh JC, Lee L, Zhang L, Wefer S, Brown K, DeRossi C, Wines ME, Rosenquist T, Holdener BC. Mesd encodes an LRP5/6 chaperone essential for specification of mouse embryonic polarity. Cell. 2003; 112:355–367. [PubMed: 12581525]

Huang H, He X. Wnt/beta-catenin signaling: new (and old) players and new insights. Curr Opin Cell Biol. 2008; 20:119–125. [PubMed: 18339531]

Jeon H, Meng W, Takagi J, Eck MJ, Springer TA, Blacklow SC. Implications for familial hypercholesterolemia from the structure of the LDL receptor YWTD-EGF domain pair. Nat Struct Biol. 2001; 8:499–504. [PubMed: 11373616]

Johnson BA. Using NMRView to visualize and analyze the NMR spectra of macromolecules. Methods Mol Biol. 2004; 278:313–352. [PubMed: 15318002]

Koduri V, Blacklow SC. Requirement for natively unstructured regions of mesoderm development candidate 2 in promoting low-density lipoprotein receptor-related protein 6 maturation. Biochemistry. 2007; 46:6570–6577. [PubMed: 17488095]

Kohler C, Andersen OM, Diehl A, Krause G, Schmieder P, Oschkinat H. The solution structure of the core of mesoderm development (MESD), a chaperone for members of the LDLR-family. J Struct Funct Genomics. 2006; 7:131–138. [PubMed: 17342452]

Lambert C, Leonard N, De Bolle X, Depiereux E. ESyPred3D: Prediction of proteins 3D structures. Bioinformatics. 2002; 18:1250–1256. [PubMed: 12217917]

Lee D, Walsh JD, Mikhailenko I, Yu P, Migliorini M, Wu Y, Krueger S, Curtis JE, Harris B, Lockett S, et al. RAP uses a histidine switch to regulate its interaction with LRP in the ER and Golgi. Mol Cell. 2006; 22:423–430. [PubMed: 16678114]

Li Y, Chen J, Lu W, McCormick LM, Wang J, Bu G. Mesd binds to mature LDL-receptor-related protein-6 and antagonizes ligand binding. J Cell Sci. 2005; 118:5305–5314. [PubMed: 16263759]

Li Y, Lu W, He X, Schwartz AL, Bu G. LRP6 expression promotes cancer cell proliferation and tumorigenesis by altering beta-catenin subcellular distribution. Oncogene. 2004; 23:9129–9135. [PubMed: 15516984]

Liu CC, Pearson C, Bu G. Cooperative folding and ligand-binding properties of LRP6 beta-propeller domains. J Biol Chem. 2009; 284:15299–15307. [PubMed: 19339249]

May P, Herz J, Bock HH. Molecular mechanisms of lipoprotein receptor signalling. Cell Mol Life Sci. 2005; 62:2325–2338. [PubMed: 16158188]

Noll G, Avola M, Lynch M, Daub J. Comparison of Alternant and Nonalternant Aromatic Bridge Systems with Respect to Their ET-Properties. The Journal of Physical Chemistry C. 2007; 111:3197–3204.

Sivashanmugam A, Wang J. A unified scheme for initiation and conformational adaptation of human apolipoprotein E N-terminal domain upon lipoprotein binding and for receptor binding activity. J Biol Chem. 2009; 284:14657–14666. [PubMed: 19307174]

Stevens FJ, Argon Y. Protein folding in the ER. Semin Cell Dev Biol. 1999; 10:443–454. [PubMed: 10597627]

Strickland DK, Gonias SL, Argraves WS. Diverse roles for the LDL receptor family. Trends Endocrinol Metab. 2002; 13:66–74. [PubMed: 11854021]

Zhang Y, Wang Y, Li X, Zhang J, Mao J, Li Z, Zheng J, Li L, Harris S, Wu D. The LRP5 high-bone-mass G171V mutation disrupts LRP5 interaction with Mesd. Mol Cell Biol. 2004; 24:4677–4684. [PubMed: 15143163]

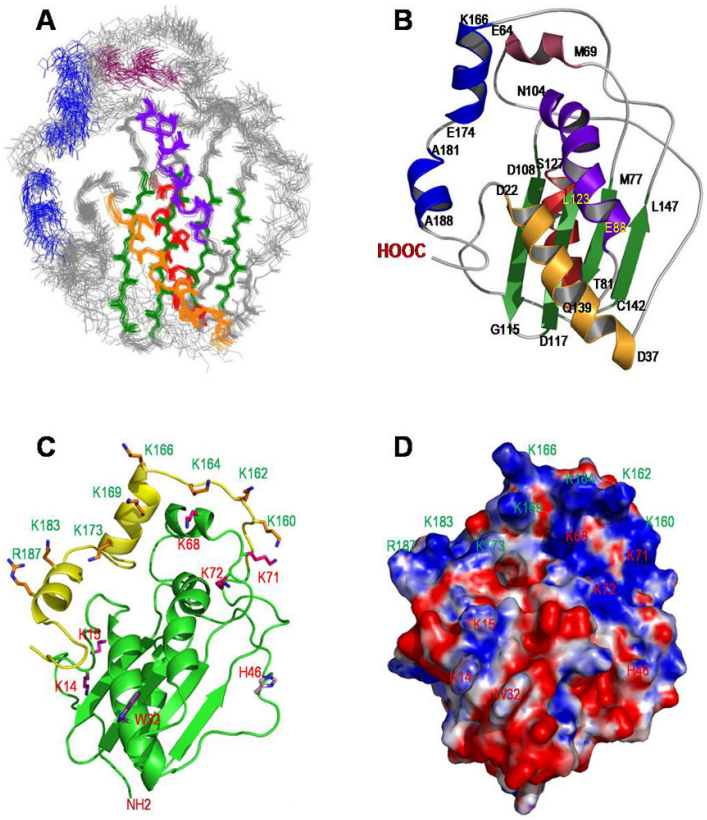

Figure 1. NMR Structure of Mouse MESD

(A) The superposition of the 20 best-fit NMR structures of mouse MESD. The superposition is based on the most conserved and rigid secondary structure region. The β-strands are colored in green, the loops are in grey and αhelices are in other colors. (B) A ribbon representation of the average structure of mouse MESD using Pymol. The colors are coded the same as (A). (C) The same ribbon representation as (B). The core domain is colored in green and the flexible C-terminal helical domain is in yellow. The sidechain heavy atoms of the key residues in both domains are highlighted using sticks and labeled in red for the core domain and in light green for the flexible helical domain. (D) Surface representation of the average NMR structure of mouse MESD, with negatively charged surface in red and positively charged surface in blue. The electrostatic potential is calculated using APBS and the surface is displayed using Pymol. The same orientation and position of MESD are shown as (C). The key residues in both domains are also labeled as (C). See also Figure S2.

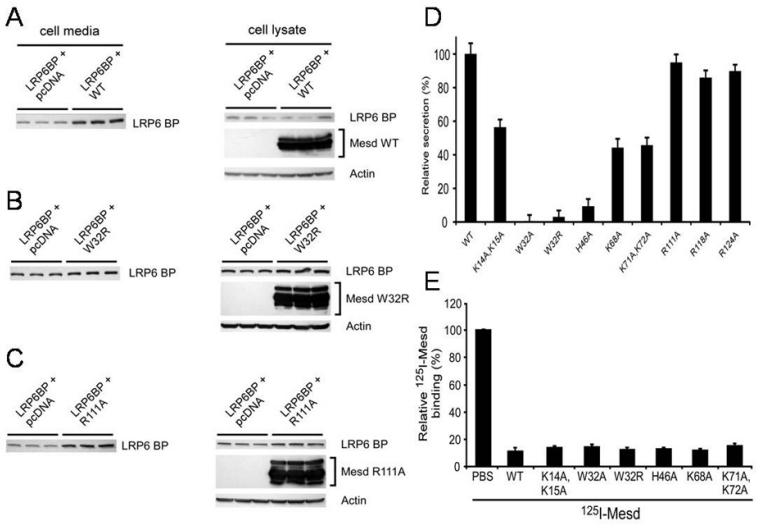

Figure 2. Identification of the Critical Residues in the Central Core Domain of MESD for Its Chaperone Function

(A) The chaperone function of the wild type MESD is demonstrated as more mature BP domain of LRP6 is secreted into medium compared with pcDNA transfection (Left). As a control, an equal amount of BP domain is observed in the cell lysate as compared with pcDNA transfection (Right). Another control for equal loading is the actin in the cell lysate. (B) Impaired chaperone function of a typical mutant, MESD_W32R. (C) Normal chaperone function of MESD_R111A. (D) Quantification of the Western blot results of different mutants, showing the relative secretion of BP domain of LRP6 after subtraction of the values from pcDNA-transfected cells. The secretion of the BP domain promoted by the wild type MESD was set at 100%. (E) Cell surface binding analyses of ^{125}I-MESD (5 nM) to LRP6-transduced HT1080 cells. MESD mutants that have the impaired chaperone function were selected for the binding competition with wildtype MESD (50 nM). In both (D) and (E), values are the means of triplicates with the standard deviation indicated by error bars. See also Figure S1.

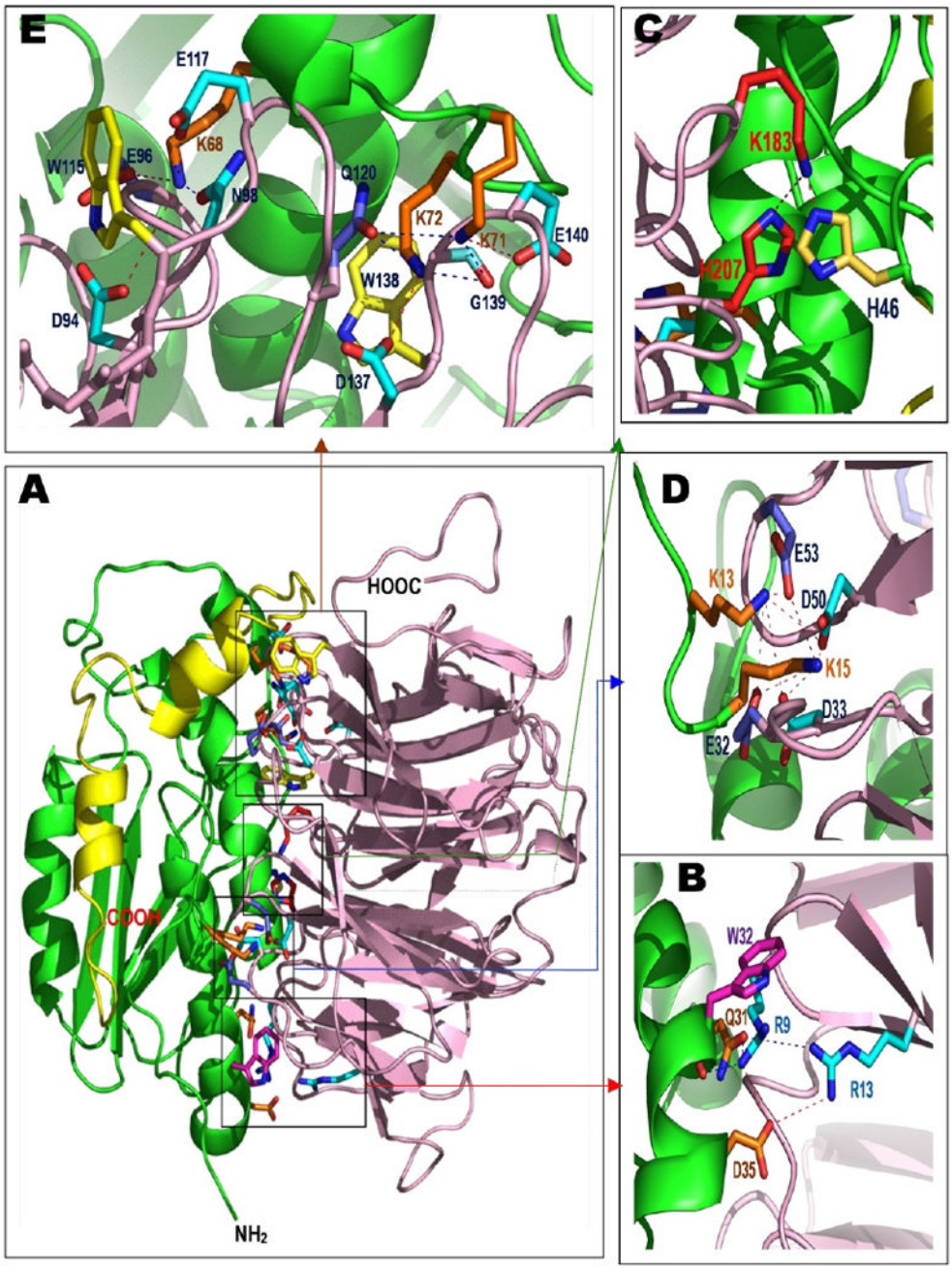

Figure 3. Possible Interaction Modes of the Chaperone Complex

(A) An overview of the chaperone complex. The chaperone domain is in green and the C-terminal flexible helical domain of MESD is in yellow. The BP domain of LRP6 is shown in pink. The sidechain atoms of the interacting residues in BP domain are shown in either blue or yellow sticks, whereas the interacting residues in MESD are shown in either brown or purple sticks. (B) Binding interface between Q31, W32, D35 in MESD and R9 and R13 in the BP domain. (C) An aromatic bridge between H46 of MESD and H207 of the BP domain. (D) Binding interface between K13, K15 of MESD and E32, D33, D50, E53 of the BP domain. (E) Binding interface between K68, K71 and K72 in MESD and D94/E96/N98/W115/E117 and Q120/D137/W138/G139/E140 in the BP domain. In (B–E), the salt bridges

are indicated with red dashed lines and H-bonds are shown with blue dashed lines. See also Figure S4.

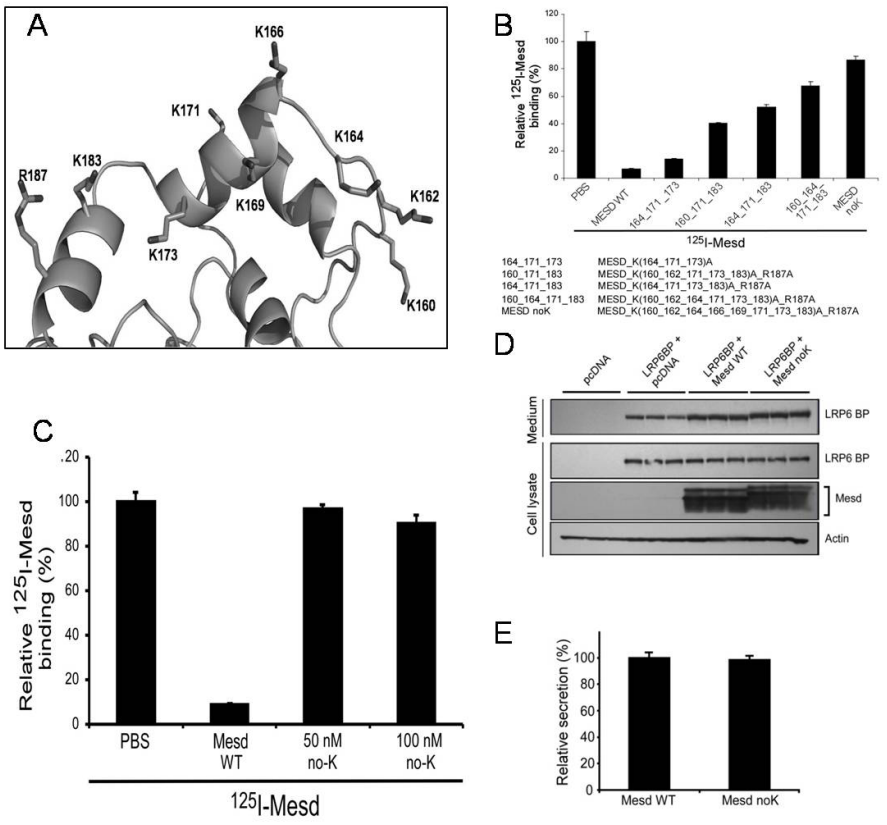

Figure 4. Identification of the Critical Residues in the C-terminal Flexible Domain of MESD for Its Escort Function

(A) Ribbon representation of the C-terminal flexible helical domain of MESD with the conserved lysine and arginine sidechain heavy atoms highlighted by sticks. (B) Competition binding results of different K or R mutations in the C-terminal flexible domain of MESD as compared with the wild-type protein, showing the binding ability of the MESD mutants to the mature, cell surface located, intact LRP6. The details of all the mutations are list underneath. (C) Competition binding results of different concentrations of the noK mutant of MESD as compared with the wild-type protein. (D) A comparison of relative secretion of the BP domain of LRP6 into the cell culture medium promoted by the noK mutant and wild-type MESD, as monitored by a Western blot of both the cell culture medium and cell lystate. (E) Quantification of the Western blot results shown in (D). In (B), (C) and (E), values shown are the means of triplet results with the standard deviation indicated by error bars. See also Figure S1.

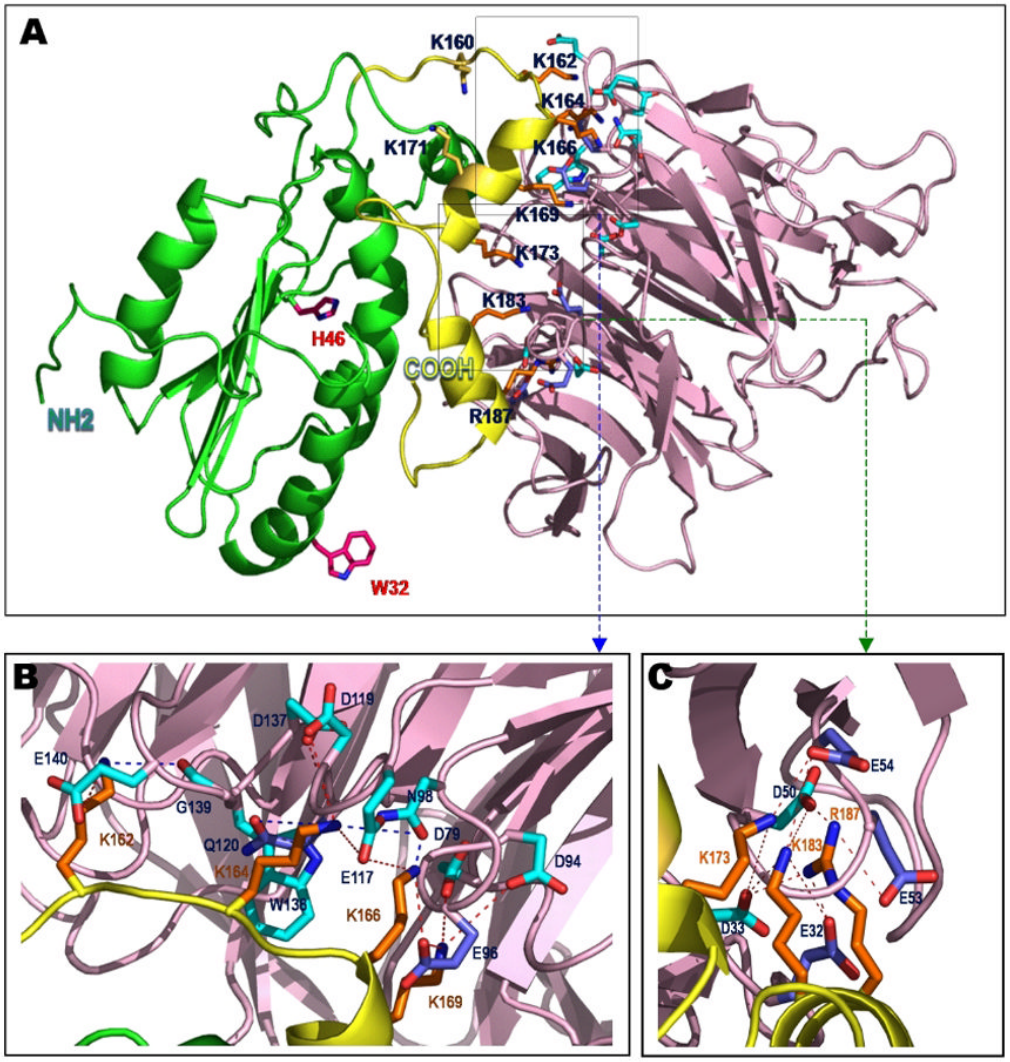

Figure 5. Possible Interaction Modes of the Escort Complex

(A) An overview of the escort complex. The chaperone domain of MESD is shown in green and the escort domain of MESD is shown in yellow. The first BP domain of LRP6 is shown in pink. The sidechain heavy atoms of the interacting residues in the BP domain are shown in blue sticks, whereas the interacting residues in MESD are shown in brown sticks. (B) Binding interfaces between K162, K164 in MESD and D119/Q120/D137/W138/G139/E140 in the BP domain, and between K166, K169 in MESD and D79/D94/E96/N98/E117 in the BP domain. (C) Binding interface between K173, K183, R187 in MESD and E32/D33/D50/E53/E54 in the BP domain. In (B) and (C), the salt bridges are indicated with red dashed lines and H-bonds are shown with blue dashed lines. See also Figure S4.

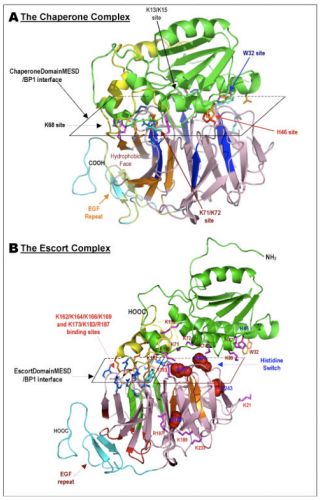

Figure 6. Structural Mechanism of MESD's Chaperone and Escort Functions

(A) The chaperone complex. For MESD, the chaperone domain is in green ribbon and the escort domain is in yellow ribbon. The BP domain is in pink with the YWTD motifs highlighted in blue, whereas the EGF repeat is in light blue. The hydrophobic interface between the β-propeller and the EGF is labeled as "Hydrophobic Face". The hydrophobic faces of the β-propeller are in brown and the hydrophobic faces of the EGF are in lemon. In this panel, five major interaction sits are labeled and highlighted with the stick models of the side chains of the interacting residues. (B) The escort complex. The colors are the same as A, except the hydrophobic interface between the β-propeller and the EGF is highlighted in red. In addition, three YWTD-motifs in the binding interface between the escort domain of MESD and the BP domain of LRP6 are colored in green, whereas the other three YWTD-motifs with the histidine switch are colored in brown. The major interaction sites are labeled and highlighted with the stick models of the side chains of the interacting residues. The interacting lysine residues in MESD are colored in brown and the interacting residues in the BP domain are colored in blue. A histidine switch is also displayed with the highlight of three histidine residues of the BP domain, H207, H226 and H243, in a space-filling model. The surrounding lysine residues in MESD are displayed as pink sticks and labeled. See also Figure S4.

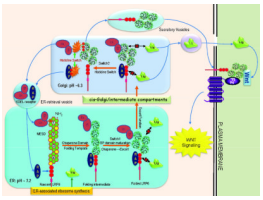

Figure 7. The MESD/LRP5/6 Pathway

The rigid chaperone domain (Ch) of MESD binds to the newly synthesized BP domain of LRP6, serving as a folding template. After BP domain properly folded, MESD switches the binding from the rigid chaperone domain to the flexible escort domain (Es), safely guarding the mature receptor traveling from the ER to the Golgi, preventing premature ligand (Lig) binding. The acidic environment of the Golgi activates the histidine switch in the BP domain that leads to the dissociation of MESD from the receptor. MESD will be retrieved back to the ER by the KDEL-receptor. The properly folded receptor will be properly post-translationally modified and further reach the cell membrane for activation of canonical WNT pathway. RAP goes through a similar cycle for promoting the ligand-binding domain folding and trafficking as described before (Herz and Marschang, 2003).

Table 1

Structural Statistics of the 20 Best-fit NMR Structures of MESD.

Number of NMR constraints		
Total NOE constraints	1646	
Intra-residue	171	
Sequential (|i − j | = 1)	510	
Medium range (1< | i − j | < 5)	568	
Long range (| i − j | > 5)	397	
Inter-domain[a]	84	
NOE constraints per residue	8.4	
Restricting long-range constraints per residue	2.0	
Number of dihedral angle restraints	264	
Number of hydrogen bonds	75	
Structural Statistics		
Distance violations (> 0.1Å, %)	0.13	
Distance violations > 0.2 Å	1	
Average Distance violations ± rmsd	0.0062±0.0013	
Dihedral angle violations (> 2.5°,%)	0.21	
Dihedral angle violations > 5°	1	
Average Dihedral angle violations ± rmsd	0.3204±0.0905	
Deviation from idealized geometry		
Bond lengths (Å)	0.0034±0.0002	
Bond angles (°)	0.2849±0.0100	
Impropers (°)	0.0676±0.0033	
Ramachandran plot (%) from Procheck	Ordered [b]	Secondary [c]
Residues in most favored regions	73.9	94.2
Residues in additional allowed regions	22.8	5.8
Residues in generally allowed regions	3.3	0.0
Residues in disallowed regions	0.0	0.0
MolProbity Clashscore	17.8	
RMSD for most conserved secondary structure region from the averaged coordinates(22–36,77–81,88–103,108–114,117–123,127–138,142–146)		
Backbone heavy atoms	0.43±0.04	
All heavy atoms	1.17±0.10	

See also Figure S3 and Table S1.

[a] Chaperone domain: residues 1–155, Escort domain: residues 156–195.

[b] Residues selected in the ordered region based on: Dihedral angle order parameter, with S(phi)+S(psi)>=1.8 Selected residue ranges: 8–38, 48–56, 63–71, 74–114, 118–148, 153–155, 159–177, 182–188, 190–194.

[c] Secondary Structure Element ranges: 22–36, 65–69, 77–81, 88–101, 108–114, 117–123, 127–139, 142–146, 166–174, 182–188